Amplitude Death in Coupled Thermoacoustic Oscillators

Tetsushi Biwa and Satoshi Tozuka
Department of Mechanical Systems and Design, Tohoku University, Sendai 980-8579, Japan

Taichi Yazaki
Department of Physics, Aichi University of Education, Kariya 448-8542, Japan

(Received 21 December 2014; published 16 March 2015)

In order to develop a simple method for preventing unwanted thermally driven acoustic gas oscillations, the amplitude-death phenomenon in thermoacoustic oscillators coupled by dissipative and time-delay coupling is experimentally studied. The coupling is designed and built using a needle valve and a half-wavelength tube. Experimental bifurcation diagrams show that oscillations can be completely stopped even in a system comprising identical oscillators when the oscillators are coupled by both dissipative and time-delay coupling. The effectiveness of this type of coupling is confirmed by numerical calculations.

DOI: 10.1103/PhysRevApplied.3.034006

I. INTRODUCTION

When two self-sustained oscillators with different natural frequencies are coupled together, *mutual synchronization* occurs and they start to oscillate with the same frequency [1]. However, with certain combinations of the coupling type and frequency detuning, *amplitude death* via stabilization to a fixed point of the dynamical system can occur [2–4]. In amplitude death, the two oscillators stop completely, in contrast to the suppression of a forced oscillator, where the natural oscillation is quenched but the forcing oscillation never vanishes [5]. The first observation of amplitude death (AD) was made in a system of two organ pipes standing side by side [6]. This problem has recently been revisited by Abel *et al.* [7,8] with a detailed mathematical description. The oscillator system that we aim to stop consists of the acoustic oscillations of a gas column (*thermoacoustic oscillations*) maintained by heat [9] rather than by the steady gas flow in organ pipes.

A lean premixed combustion is the key technology for reducing NO_x and CO emissions from gas turbine engines but is prone to generating unwanted strong gas oscillations that can cause serious damage leading to reduced lifetimes or even destruction of the engine [10]. Complete elimination of oscillations is, therefore, a strong requirement for the safe operation of aircraft and power generators. So far, passive controls have been attempted, but a simpler method is needed. In this paper, we experimentally demonstrate a strategy based on AD to suppress the oscillations.

Theoretical studies have found several types of couplings leading to AD [11]. Among them, we specifically focus on *dissipative coupling* and *time-delay coupling*. In the case of dissipative coupling, AD occurs when the frequency detuning between the oscillators is sufficiently large [12]. In the case of time-delay coupling, the oscillations are damped for suitable values of delay time and coupling strength even in a system of identical oscillators [13]. In electrical circuits, a resistor and a digital delay line provide a means of realizing these couplings [4]. In thermoacoustic systems, however, there has been no experimental evidence of AD, although forced synchronization [14–17], quenching by external forcing [5,18], and mutual synchronization [19] have been observed and analyzed. We report on the design and construction of dissipative and delayed couplings in a real acoustic system.

II. EXPERIMENT SETUP

Figure 1(a) shows the thermoacoustic oscillator (oscillator 1) used in this study. It consists of a 720-mm-long cylindrical tube with an internal diameter of 24 mm and a porous material, which is referred to as a stack. The tube is closed by rigid plates at the ends and is filled with a working fluid of air at ambient pressure and temperature. The stack is a 20-mm-long cylindrical honeycomb catalyst with a diameter such that it fits into the resonator. The square pore size of the stack is 0.93×0.93 mm^2, and the porosity is 80.0%. The stack is sandwiched between hot

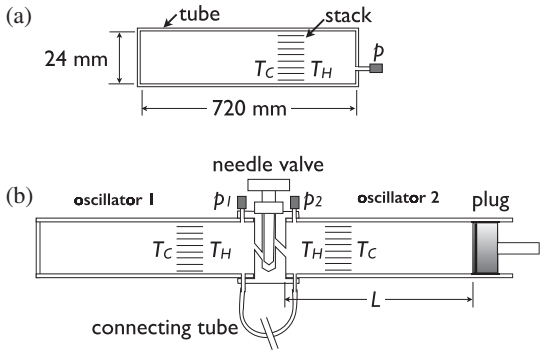

FIG. 1. Experiment setup. Thermoacoustic oscillator (a) and coupled oscillators (b) using a needle valve and a connecting tube.

and cold heat exchangers, both of which are made of cylinders with parallel plates inside of them. An electrical heater and a cooling water pipe are wound around the hot and cold heat exchangers, respectively. The hot end temperature T_H of the stack is monitored by a thermocouple and controlled by the electrical heater current, and the cold end temperature T_C is maintained at 293 K during the experiments.

When the thermoacoustic oscillator is driven away from equilibrium by the increasing control parameter $\Delta T = T_H - T_C$ [20], acoustic oscillations of the gas column begin with $\Delta T > 230$ K. The oscillation is in the fundamental acoustic mode having acoustic pressure maxima at the ends of the tube. The pressure amplitude measured with a pressure transducer mounted on the end plate of the resonator reaches 1.4 kPa with a frequency $f_1 = 250$ Hz when $\Delta T = 350$ K.

A second oscillator (oscillator 2) is built in the same way as the oscillator shown in Fig. 1(a) but with one of the end plates replaced by a brass plug sealed by an O ring to adjust the frequency f_2 of this oscillator. The detuning $\Delta f = f_2 - f_1$ between oscillators 1 and 2 is gradually changed in the range of -15 Hz $\leq \Delta f \leq 15$ Hz in steps of 2.5 Hz.

Dissipative coupling of the two oscillators is achieved by connecting them together using a needle valve (KITZ 260K-3/4). The coupling strength is controlled by the valve opening angle Φ. For the time-delay coupling, we use a vinyl tube of 4-mm internal diameter as shown in Fig. 1(b). The delay time is controlled by the length of the tube, since the acoustic fluctuation in one oscillator arrives at the other after a time proportional to this length.

In order to map out the bifurcation diagram of the coupled thermoacoustic oscillators, we record the acoustic pressures $p_1(t)$ and $p_2(t)$ near the ends of the oscillators with an analog-to-digital convertor and obtain their instantaneous amplitudes and phases from the analytical signals obtained via their Hilbert transforms [1]. During the experiments, ΔT for oscillator 1 is maintained at 350 K. For oscillator 2, ΔT is adjusted so that the acoustic pressure amplitude of $p_2(t)$ becomes the same as that of $p_1(t)$ when the coupling is off and is maintained after the coupling is turned on. Pressure measurements are taken after the system reaches a steady state.

III. RESULTS AND DISCUSSION

The two-parameter bifurcation diagram for the dissipatively coupled oscillators is mapped in Fig. 2(a) with the valve opening angle Φ and the frequency detuning Δf as parameters. The evolution of the oscillatory dynamics along route A with $\Delta f = 5$ Hz is shown in Fig. 2(b), where the pressure amplitude P_1 of $p_1(t)$ and the phase difference θ between $p_1(t)$ and $p_2(t)$ are illustrated as functions of Φ. The Φ dependence of P_2 of $p_2(t)$, not shown in Fig. 2(a) for brevity, is almost the same as P_1. For the relatively small values of Φ in region (I), a quasiperiodic

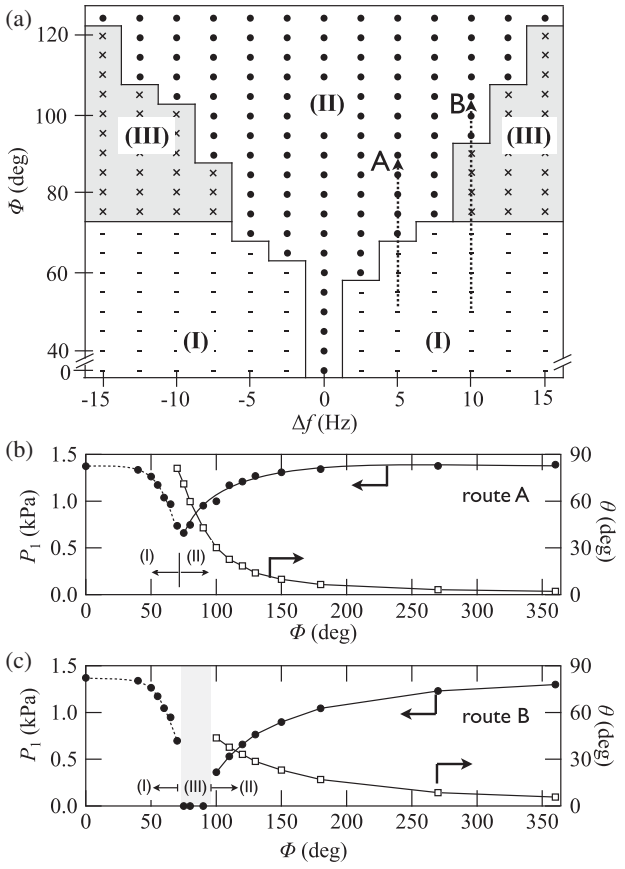

FIG. 2. Two-parameter bifurcation diagram (a) when thermoacoustic oscillators are coupled by the valve. The pressure amplitude P_1 and phase difference θ between oscillators 1 and 2 as functions of the valve opening Φ when the detuning Δf is 5 Hz (b) and 10 Hz (c). Regions (I), (II), and (III) denote asynchronous states, synchronous states, and amplitude death, respectively.

motion on a torus is observed. The amplitude P_1 time averaged over a beat period gradually decreases with increasing Φ, but it starts to increase at $\Phi = 75°$ in response to the *saddle-node bifurcation* to the synchronization region (II) with $\Phi > 75°$. With further increases in Φ, the instantaneous phase difference θ of $p_2(t)$ relative to $p_1(t)$ approaches zero (in-phase synchronization), and at the same time, the amplitude P_1 returns to the value it had without coupling when $\Phi = 0$.

When we follow route B in Fig. 2(a) with the detuning $\Delta f = 10$ Hz, P_1 decreases with increasing Φ, as observed in the case with $\Delta f = 5$ Hz, but the torus bifurcates to the fixed point at $\Phi = 75°$, showing the appearance of AD. The zero-amplitude state persists until the synchronous state appears with $\Phi > 95°$ through a Hopf bifurcation.

The presence of AD in the intermediate region of Φ between 75° and 90° is reasonable from the energetic point of view. The reciprocating gas parcels through the abrupt changes of cross section at the inlet and outlet of the valve cause a *minor loss* of acoustic power due to vortex

generation [21]. If Φ is small, this loss is small as the resulting gas flow rate is low, but the loss should increase with Φ and thereby reduce the oscillation amplitude to zero. At higher Φ, however, the oscillations recover because the stronger coupling leads to in-phase synchronization which prevents gas flow through the valve as $p_1(t) = p_2(t)$ holds. In other words, it is hard to suppress oscillations when identical thermoacoustic oscillators with $\Delta f = 0$ are dissipatively coupled through a needle valve only because in-phase synchronization easily takes place.

The time-delay coupling is tested with the valve completely closed ($\Phi = 0$) while keeping the detuning $\Delta f = 0$ and $\Delta T = 350$ K. When the two oscillators are connected by a 600-mm-long tube close to a half-wavelength, antiphase synchronization is realized, as observed by Spoor and Swift [19]. Synchronization will introduce AD more easily, because it makes the pressure difference $p_2(t) - p_1(t)$ across the valve large. So if such phasing is maintained when the valve is opened, the gas flow rate and the associated energy loss should be enhanced. Therefore, we connect oscillators 1 and 2 together using both the needle valve and the half-wavelength tube, as shown in Fig. 1(b).

Figures 3(a) and 3(b) present $p_1(t)$ and $p_2(t)$ observed in the coupled oscillators with $\Delta f = 0$. In Fig. 3(a), Φ changes from 0° to 80° at $t = 0$ after antiphase synchronization is achieved in advance via the tube. It can be seen that $p_1(t)$ and $p_2(t)$ oscillating 180° out of phase with each other gradually decrease to zero after a time, which signifies the stabilization at a fixed point with zero amplitude. Figure 3(b) shows the case when the tightly pinched tube is released at $t = 0$ after the in-phase synchronization is achieved by the valve ($\Phi = 80°$). We see that the AD occurs irrespectively of which coupling is turned on first, although the relaxation times for the oscillation decay are different in Figs. 3(a) and 3(b).

Through further observations of $p_1(t)$ and $p_2(t)$ with various Δf and Φ, we create the bifurcation diagram shown in Fig. 3(c). The death region (III) extends over a much wider area than that obtained with dissipative coupling via the needle valve in Fig. 2(a). Also, we see that the oscillation stops for all values of Δf with $\Phi \geq 60°$, while the oscillation survives in the range of -7.5 Hz $\leq \Delta f \leq 10.0$ Hz when the valve is closed ($\Phi = 0$). This result means that the present tube coupling is not sufficiently strong to stop the oscillations without the valve coupling, although Reddy *et al.* [4] succeeded in suppressing oscillations in electrical circuits by time-delay coupling alone. In other words, our results indicate that AD more easily occurs when dissipative coupling is combined with time-delay coupling. In order to verify the effectiveness of this type of coupling, we present some numerical calculation results below.

We consider Van der Pol oscillators mutually coupled by dissipative and time-delay coupling,

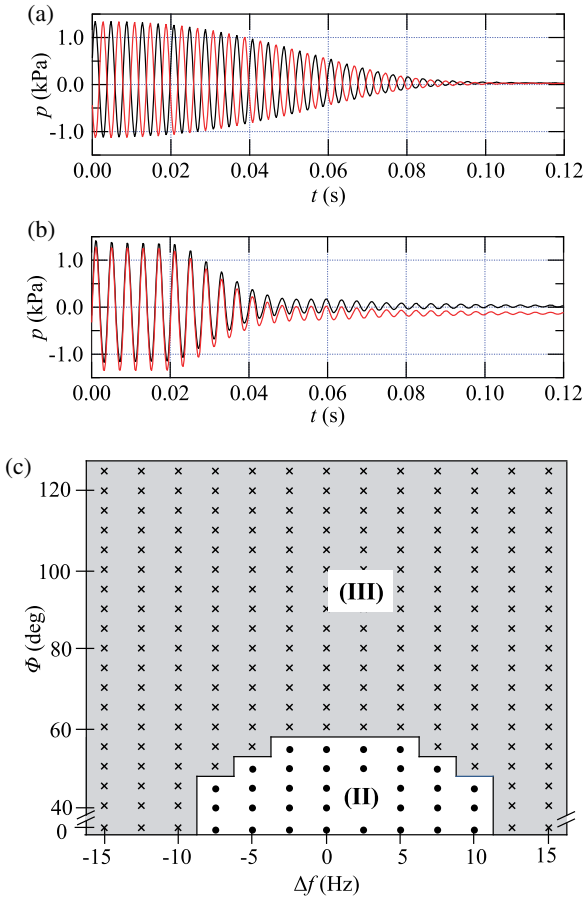

FIG. 3. Temporal variation of the acoustic pressures $p_1(t)$ (red) and $p_2(t)$ (black) in the coupled oscillators with $\Delta f = 0$, (a) when the valve is open at $t = 0$ after the antiphase synchronous state is achieved via the connecting tube, and (b) when the tube is open at $t = 0$ after the in-phase synchronous state is achieved via the valve. (c) Two-parameter bifurcation diagram when the thermoacoustic oscillators are coupled by both the valve and the tube. Regions (II) and (III) denote the synchronous state and amplitude death, respectively.

$$\ddot{x}_i - (\epsilon_i - x_i^2)\dot{x} + \omega_i^2 x_i = K_d(\dot{x}_j - \dot{x}_i) + K_\tau[\dot{x}_j(t-\tau) - \dot{x}_i(t)], \quad (1)$$

where $i, j = 1, 2$ and $i \neq j$. The first term on the right-hand side of Eq. (1) represents dissipative coupling with strength K_d, whereas the second term represents the time-delay coupling with strength K_τ and delay time τ. Inserting $K_\tau = 0$ reduces the dynamical system of Eq. (1) to dissipatively coupled oscillators [22], while $K_d = 0$ yields time-delay coupled ones. In Figs. 4(a) and 4(b), we present the numerical bifurcation diagrams for dissipative coupling ($K_\tau = 0$) and dissipative coupling plus time-delay coupling ($K_\tau = 0.04$), where the parameters are taken as $\epsilon_1 = \epsilon_2 = 0.03$, $\omega_1 = 1$, and $\tau = 3.1$, which is close to half the natural period. We see a close resemblance to the experimental bifurcation diagrams in Figs. 2(a) and 3(c), where the plot range of $0.94 < \omega_2/\omega_1 < 1.06$ of Figs. 4(a)

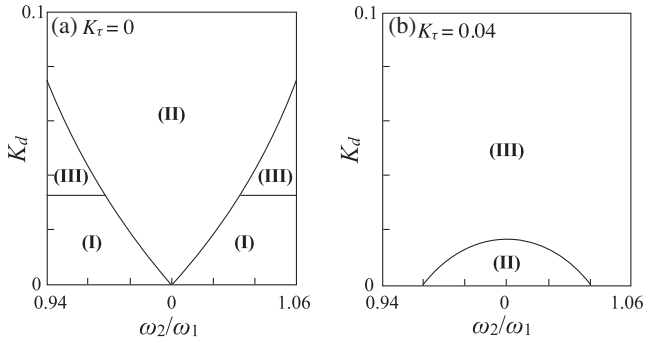

FIG. 4. Bifurcation diagrams of Van der Pol oscillators coupled by (a) dissipative coupling and (b) by both dissipative and time-delay coupling. Regions (I), (II), and (III) denote asynchronous states, synchronous states, and amplitude death, respectively.

and 4(b) corresponds to the range of Δf in the experiments (-15 Hz $< \Delta f <$ 15 Hz). If the valve opening angle Φ is proportional to K_d, the threshold value of $\Phi = 75^\circ$ at the boundary between regions (I) and (III) will correspond to $K_d = 0.035$. Figures 4(a) and 4(b) indicate that mutually coupled Van der Pol oscillators can reproduce the present system, although the hydrodynamic equations governing thermoacoustic oscillators are far more complicated than Eq. (1) [23].

Finally, we carry out a numerical investigation of the effectiveness of valve-tube coupling by varying the values of K_τ and τ while keeping $\omega = \omega_i = 1$ ($i = 1, 2$). Figure 5(a) shows the bifurcation diagram for time-delay coupling with $K_d = 0$ in Eq. (1), where the death islands are located near $\omega\tau = \pi/2$ and $\omega\tau = 3\pi/2$ as observed by Reddy *et al.* [4]. Shown in Fig. 5(b) is the bifurcation diagram for time-delay coupling plus dissipative coupling with $K_d = 0.02$. We see that the death island centered at $\omega\tau = \pi$ extends to a much wider area including $K_\tau \approx 0.02$. As shown in Fig. 4(a), the coupling strength $K_d = 0.02$ is well below the threshold value for AD to occur by dissipative coupling alone. This result demonstrates that AD can occur under dissipative coupling plus time-delay coupling even when the coupling strengths are considerably weak, lending support to the experimental results.

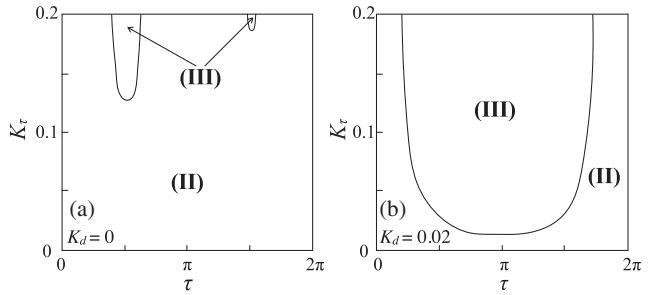

FIG. 5. Bifurcation diagrams of (a) time-delay coupling with $K_d = 0$ and (b) dissipative coupling ($K_d = 0.02$) plus time-delay coupling. Regions (II) and (III) denote synchronous states and amplitude death, respectively.

IV. SUMMARY

In summary, we demonstrate the amplitude-death phenomenon in thermoacoustic oscillators coupled by dissipative and time-delay coupling. These couplings are realized using a needle valve alone and using both a needle valve and a half-wavelength tube. The experimental bifurcation diagrams show the valve-tube coupling to be more capable than tube coupling alone for annihilating oscillations. The amplitude-death phenomenon can become a powerful tool for preventing unwanted oscillations in thermoacoustic systems. We plan to use the proposed technique to suppress unstable oscillations in real combustion systems.

ACKNOWLEDGMENTS

This work is supported by JSPS KAKENHIs (Grant No. 26286073 to T. B. and Grant No. 25400398 to T. Y.).

[1] A. Pikovsky, M. Rosenblum, and J. Kurth, *Synchronization: A Universal Concept in Nonlinear Sciences* (Cambridge University Press, Cambridge, England, 2001).
[2] P. C. Matthews and S. H. Strogatz, Phase Diagram for the Collective Behavior of Limit-Cycle Oscillators, Phys. Rev. Lett. **65**, 1701 (1990).
[3] R. Herrero, M. Figueras, J. Rius, F. Pi, and G. Orriols, Experimental Observation of the Amplitude Death Effect in Two Coupled Nonlinear Oscillators, Phys. Rev. Lett. **84**, 5312 (2000).
[4] D. V. R. Reddy, A. Sen, and G. L. Johnston, Experimental Evidence of Time-Delay-Induced Death in Coupled Limit-Cycle Oscillators, Phys. Rev. Lett. **85**, 3381 (2000).
[5] B. D. Bellows, A. Hreiz, and T. Lieuwen, Nonlinear interactions between forced and self-excited acoustic oscillations in premixed combustor, J. Propul. Power **24**, 628 (2008).
[6] J. W. S. Rayleigh, *The Theory of Sound* (Dover, New York, 1945), Vol. 2.
[7] M. Abel, S. Bergweiler, and R. Gerhard-Multhaupt, Synchronization of organ pipes: Experimental observations and modeling, J. Acoust. Soc. Am. **119**, 2467 (2006).
[8] M. Abel, K. Ahnert, and S. Bergweiler, Synchronization of Sound Sources, Phys. Rev. Lett. **103**, 114301 (2009).
[9] G. W. Swift, Thermoacoustic engines, J. Acoust. Soc. Am. **84**, 1145 (1988).
[10] C. J. Goy, S. R. James, and S. Rea, in *Combustion Instabilities in Gas Turbine Engines: Operational Experience, Fundamental Mechanism, and Modeling*, Progress in Astronautics and Aerodynamics, edited by T. C. Lieuwen and V. Yang (American Institute of Aeronautics and Astronautics, Reston, VA, 2005), Chap. 8.
[11] G. Saxena, A. Prasad, and R. Ramaswamy, Amplitude death: The emergence of stationarity in coupled nonlinear systems, Phys. Rep. **521**, 205 (2012).

[12] D. G. Aronson, G. B. Ermentrout, and N. Kopell, Amplitude response of coupled oscillators, Physica (Amsterdam) **41D**, 403 (1990).

[13] D. V. R. Reddy, A. Sen, and G. L. Johnston, Time Delay Induced Death in Coupled Limit Cycle Oscillators, Phys. Rev. Lett. **80**, 5109 (1998).

[14] T. Yoshida, T. Yazaki, Y. Ueda, and T. Biwa, Forced synchronization of periodic oscillations in a gas column: Where is the power source?, J. Phys. Soc. Jpn. **82**, 103001 (2013).

[15] G. Penelet and T. Biwa, Synchronization of a thermoacoustic oscillator by an external sound source, Am. J. Phys. **81**, 290 (2013).

[16] L. K. B. Li and M. P. Juniper, Phase trapping and slipping in a forced hydrodynamically self-excited jet, J. Fluid Mech. **735**, R5 (2013).

[17] S. Balusamy, L. K. B. Li, Z. Han, M. P. Juniper, and S. Hochgreb, Nonlinear dynamics of a self-excited thermoacoustic system subjected to acoustic forcing, Proc. Combust. Inst. **35**, 3229 (2015).

[18] T. Yazaki, Experimental observation of thermoacoustic turbulence and universal properties at the quasiperiodic transition to chaos, Phys. Rev. E **48**, 1806 (1993).

[19] P. S. Spoor and G. W. Swift, Mode-locking of acoustic resonators and its application to vibration cancellation in acoustic heat engines, J. Acoust. Soc. Am. **106**, 1353 (1999).

[20] T. Biwa, F. Shima, and T. Yazaki, Experimental determination of the evolution equation for thermally induced acoustic oscillations, J. Phys. Soc. Am. **82**, 043401 (2013).

[21] A. Petculescu and L. A. Wilen, Oscillatory flow in jet pumps: Nonlinear effects and minor losses, J. Acoust. Soc. Am. **113**, 1282 (2003).

[22] A. Balanov, N. Janson, D. Postnov, and O. Sosnovtseva, *Synchronization: From Simple to Complex* (Springer, Berlin, 2009), Chap. 4.

[23] N. Rott, Damped and thermally driven acoustic oscillations in wide and narrow tubes, Z. Agnew. Math. Phys. **20**, 230 (1969).